ENVIRONMENTAL RESEARCH
LETTERS

PURPOSE-LED
PUBLISHING™

ACCEPTED MANUSCRIPT • OPEN ACCESS

Uncertainty in determining carbon dioxide removal potential of biochar

To cite this article before publication: Seth Kane *et al* 2024 *Environ. Res. Lett.* in press https://doi.org/10.1088/1748-9326/ad99e9

Uncertainty in determining carbon dioxide removal potential of biochar

Seth Kane [a, †], Ahmad Bin Thaneya [b], Aysegul Petek Gursel [b], Jin Fan [a], Baishakhi Bose [c], Thomas P. Hendrickson [d], Sarah L. Nordahl [d], Corinne D. Scown [c,d,e,f], Sabbie A. Miller [a], Arpad Horvath [b]

[a] Department of Civil and Environmental Engineering, University of California, Davis
[b] Department of Civil and Environmental Engineering, University of California, Berkeley
[c] Biological Systems and Engineering Division, Lawrence Berkeley National Laboratory
[d] Energy Analysis and Environmental Impacts Division, Lawrence Berkeley National Laboratory
[e] Joint BioEnergy Institute, Lawrence Berkeley National Lab
[f] Energy & Biosciences Institute, University of California, Berkeley
[†] Corresponding Author: T +1 907 750 6364, E skane@ucdavis.edu

Abstract:

A quantitative and systematic assessment of uncertainty in life-cycle assessment is critical to informing sustainable development of carbon dioxide removal (CDR) technologies. Biochar is the most commonly sold form of CDR to date, and it can be used in applications ranging from concrete to agricultural soil amendments. Previous analyses of biochar rely on modeled or estimated life-cycle data and suggest a cradle-to-gate range of 0.20 – 1.3 kg CO_2 net removal per kg of biomass feedstock, driven by differences in energy consumption, pyrolysis temperature, and feedstock sourcing. Herein, we quantify the distribution of CDR possible for biochar production with a compositional life-cycle inventory model paired with scenario-aware Monte Carlo simulation in a "best practice" (incorporating lower transportation distances, high pyrolysis temperatures, high energy efficiency, recapture of energy for drying and pyrolysis energy requirements, and co-generation of heat and electricity) and "poor practice" (higher transportation distances, lower pyrolysis temperatures, low energy efficiency, natural gas for energy requirements, and no energy recovery) scenarios. In the best-practice scenario, cradle-to-gate CDR (which is representative of the upper limit of removal across the entire life cycle) is highly certain, with a median removal of 1.4 kg of CO_2e / kg biomass and results in net removal across the entire distribution. In contrast, the poor-practice scenario results in median net emissions of 0.090 kg CO_2e / kg biomass. Whether this scenario emits (66% likelihood) or removes (34% likelihood) carbon dioxide is highly uncertain. The emission intensity of energy inputs to the pyrolysis process and whether the bio-oil co-product is used as a chemical feedstock or combusted are critical factors impacting the net carbon dioxide emissions of biochar production, together responsible for 98% of the difference between the best- and poor-practice scenarios.

Keywords:

Pyrolysis, life-cycle assessment (LCA), Monte Carlo simulation, carbon sequestration, greenhouse gas emissions.

1. Introduction

Methods to take up and store atmospheric carbon dioxide are needed to limit global warming to less than 2 °C and avoid the worst impacts of climate change.[1] Currently, the production of biochar from biomass residues via pyrolysis is the most widely applied engineered method for carbon dioxide removal (CDR)[2] and is estimated to be at a technology readiness level of 8-9,[3] which is higher than other CDR technologies such as direct-air capture.[4] Continued rapid development of CDR technologies, including

biochar, is needed to meet targets of 2.1-2.6 Gt CO_2 removal by 2030.[5] Biochar can provide additional benefits beyond CDR in applications, including as an agricultural soil amendment[6–8] or as an additive in concrete or plastics.[9,10,11,12]

Biochar production is estimated to have stored 650 kt CO_2 in 2023,[13] but reports on biochar's storage capacity vary. A comparison of 37 previous academic life-cycle inventories (LCIs) of biochar production shows a range of carbon emission values (Supplemental Table 1, negatives indicate removal): a 5th-95th percentile range of -0.20 to -1.51kg CO_2e /kg and a median CDR of -0.70 kg CO_2e/kg when normalized by functional unit (1 kg of feedstock), scope (cradle-to-gate), and allocation method (see Supplemental Information for details).[6,14–21] Differences are driven primarily by pyrolysis temperatures, with low pyrolysis temperatures resulting in high CDR (average of -1.2 kg CO_2e/kg for pyrolysis temperatures ≤ 400 °C) at the factory gate but more rapid decomposition during biochar application.[22] Using purpose-grown crops as a feedstock can reduce CDR potential (average of -0.3 kg CO_2e/kg) relative to using residual biomass (average CDR of -0.75 kg CO_2e/kg) due to energy and fertilizer impacts from primary crop production. While limited previous life-cycle assessments (LCAs) have examined fossil energy sources during pyrolysis, emissions associated with fossil fuel energy inputs can reduce CDR potential.[18] Other reported variations in carbon uptake can be driven by varying system boundaries, carbon accounting methods, and assumptions regarding land-use changes during biomass growth.[23] Finally, the treatment of pyrolysis syngas and bio-oil co-products can play a key role, with some systems producing energy from these products, some systems using bio-oil as a chemical or material feedstock or injecting it for carbon storage, and some systems flaring these energy co-products, without energy recovery.

All but one of the 37 biochar LCIs identified in the academic literature rely on process calculations,[19] kinetic models,[14] machine-learning models,[24] or compositional models[17] to estimate at least a portion of their pyrolysis LCI data. Such modeling efforts are particularly useful when specific process data are unavailable but introduce additional uncertainty.[25] The lack of comprehensive, public, real-world operational data for these processes means modeling is required to estimate life-cycle impacts, which leads to increased uncertainty.

In addition to the academic LCIs, 16 commercial CDR values were identified, either based on the Puro.earth CDR standards[26] or Environmental Product Declarations (EPDs) for biochar[27]. These commercial CDR values ranged from -0.2 to -1.22 kg CO_2e / kg feedstock, with a median of -0.65 kg CO_2e / kg (Supplemental Table 2) – a similar range to the academic LCAs, despite no harmonization. Variation in CDR from both academic and commercial approaches indicates that in addition to the uncertainty resulting from modeling approaches, there is significant variation resulting from differences in operating parameters that contribute to the total uncertainty in biochar CDR. Understanding the role of modeling uncertainty, process uncertainty, and process variations between different process parameters when examining future production scenarios is currently a critical gap in understanding the net CDR potential of biochar across the industry as a whole. When uncertainty is incorporated into decision-making, understanding the role of modeling uncertainty relative to process uncertainty (e.g., uncertainty surrounding facility-specific efficiency) and variation (e.g., different fuel mixes by country) can inform confidence in real-world CDR based on modeled data.

LCA data are fundamentally uncertain,[28] which can arise from random error, statistical variation, differences between inventory data and the actual system, geospatial variation, temporal variations, differences in scope, and differences in carbon accounting method. This uncertainty is often accounted for in LCA with Monte Carlo simulation (MCS), data quality indicators (DQIs), sensitivity analysis, and pedigree matrices.[29] Understanding the role of both variation and uncertainty in LCA results plays a critical role in the interpretation of LCA results and policy decisions based on those results.[28] Noting the

substantial range in existing CDR values, determining the degree and causes of uncertainty is critical to accurately estimating biochar CDR and energy production potential and is underrepresented in existing biochar LCAs.

In this work, we examine the role of critical production process parameters on biochar CDR potential by investigating energy and emission impacts from biochar production from wood residues with scenario-aware Monte Carlo simulation (SA-MCS)[29] paired with our previously published compositional model for predicting pyrolysis life-cycle inventory data.[17] This paired approach allows for variation and uncertainty in process parameters to be input to the LCI model, giving a quantified understanding of how uncertainty and variation in each underlying parameter, as well as uncertainty from model error, impact the resulting CDR potential of biochar. A scenario analysis comparing a "best practices" scenario to a "poor practices" scenario is then applied in conjunction with this simulation to highlight the range of CDR potential possible for current industrial processes as well as the relative impact of key factors on uncertainty and median CDR potential. By examining variation and uncertainty in biochar CDR potential from a fundamental level, this work addresses key data needs regarding the uncertainty of existing LCA data for biochar production. The results of this model provide guidance on pyrolysis process design to maximize the carbon storage of this critical CDR method.

2. Methods

2.1 Scope

In this work, we follow a life-cycle assessment (LCA) methodology with a cradle-to-gate scope, ending at the pyrolysis plant gate, for a "best practices" Scenario 1 and a "poor practices" Scenario 2 to show the range of emissions possible with pyrolysis facility designs (Figure 1). As the goal of this work is to assess CDR potential, we exclusively examine greenhouse gas emissions. We note that, as this analysis excludes the application phase, biochar stability is not considered, and therefore, the CDR values presented herein should be considered a maximum for the whole lifecycle. Two bio-oil co-product applications are modeled: bio-oil as a feedstock for chemical products (Scenario 1) and combustion without energy capture (Scenario 2). All values are reported with a functional unit of 1 kg biomass feedstock. A mass feedstock functional unit is selected due to variations in the properties of the biochar produced, which may bias results if a functional unit of mass biochar is used. Additionally, this functional unit can be used to compare these results with other alternative uses of biomass residues, such as combustion or gasification.

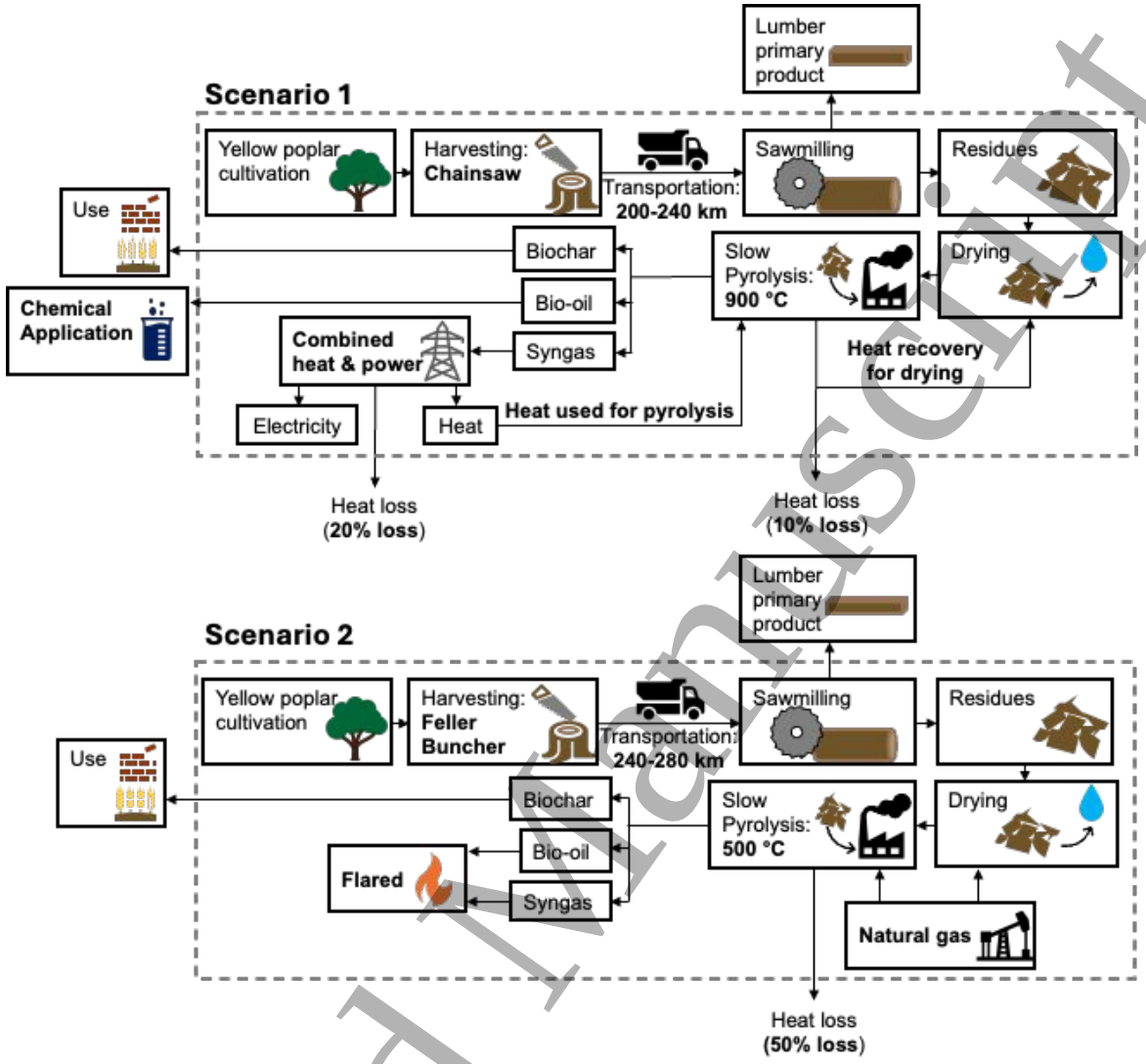

Figure 1. Scope and comparison of two examined scenarios. Differences between scenarios are bolded.

2.2 Life cycle inventory

2.2.1 Biomass growth and harvesting

We examine biochar produced from yellow poplar sawmill residues, with a range of compositions (Supplemental Table 3). Wood residues are one of the most applied biochar feedstocks,[13] and their availability is expected to grow.[30] For the impacts associated with growth and collection operations (e.g., fossil fuel use during logging), LCI data were based on published literature[31,32] and GREET[33] (See Supplemental Information). Scenario 1 (Figure 1) considers the impact of chainsaw-based harvesting (typical of smaller-sized sawmills), while Scenario 2 considers the impact of feller-buncher-based harvesting (common for medium to large-sized sawmills) during logging operations. A high- (240-280 km) and a low-emission (200-240 km) transportation scenario are examined for transporting this feedstock from the forest to the sawmill. In both cases, transportation is modeled by truck, with an emission factor of 0.157-0.169 kg CO_2e / t·km, with a uniform distribution[34].

Residues are calculated based on a median mass efficiency of 83.7% (Supplemental Figure 1). Emissions resulting from the growth, harvesting, and transportation of biomass residues from the site of harvest to sawmill were allocated to the final biochar product on a mass basis to normalize this analysis with agricultural residue feedstocks. All energy use associated with the sawmilling process is allocated to the primary lumber product, as this energy use is specific to the geometry of the final lumber product. We note that other allocation approaches could be used (e.g., no burdens assigned to residues, system expansion, or economic allocation).

2.2.2 Pyrolysis

Pyrolysis is modeled with a previously developed compositional pyrolysis model developed in our previous work.[17] This compositional model predicts whole biomass pyrolysis products for a given temperature based on the cellulose, hemicellulose, lignin, and ash composition of the biomass feedstock by additively combining the pyrolysis products of each biomass constituent. This model estimates biochar, bio-oil, and syngas yields and composition, as well as the energy requirement of pyrolysis and drying. Pyrolysis is examined with a temperature range of 880-900 °C and 490-510 °C for Scenario 1 and 2, respectively, and a heating rate of 10 °C/min for both Scenarios. In Scenario 1, a higher pyrolysis temperature was selected due to the similar bound carbon in biochar at high pyrolysis temperatures, alongside an increase in the syngas produced and increased carbon stability during the use phase due to reduced H content.[35] Uncertainty distributions from the residuals of the predictive compositional model's validation dataset are used as model uncertainty for each parameter.

The thermal efficiency of pyrolysis is considered at both a low and a high level: 50% (range of 45 – 55%) and 90% (range of 85 – 95%) efficiency.[6,24] Pyrolysis energy requirements are met with pyrolysis energy products from earlier pyrolysis reactions (Scenario 1) and the use of external energy source of natural gas (Scenario 2, emission factor of 0.0504 kg CO_2e/MJ [36], with no uncertainty in emission factor considered). Natural gas was selected for Scenario 2, as it is widely available, is considered a lower emission energy source than other fossil fuels (e.g., coal or oil), and has more limited regional variation in emission factor than electricity or biomass energy sources that have more commonly been examined previously (Supplemental Table 1).

2.2.3 Bio-oil and syngas co-products

In Scenario 1, syngas is combusted using a heat and electricity co-generation boiler (median efficiency of 50% of the lower heating value (LHV)as heat and 25% of LHVas electricity based on a review of literature data (Supplemental Table 5)[37–51]), and bio-oil is used as a feedstock for chemical products. No GHG emission credits are applied for energy production, and no allocation is performed to energy produced. All downstream processing impacts of bio-oil are allocated to the chemical product and no pyrolysis impacts are assigned to this product. We assume carbon bound in bio-oil products contributes to CDR, however, this is strongly dependent on the length of the lifespan and end-of-life scenario for this exact product. In Scenario 2, both bio-oil and syngas are flared, with no energy recovery.

Ranges of input data are given in Table 1 and complete distributions of input data and model error are shown in Supplemental Figures 1 and 3.

2.3 Scenario-aware Monte Carlo simulation

Scenario-aware Monte Carlo simulation (SA-MCS) is applied to determine the parameter, model, and scenario uncertainty of the LCA.[29] This scenario-aware approach differs from conventional LCA MCS by accounting for variation and uncertainty probability distributions at the process parameter level and,

from this uncertainty, calculating uncertainty in both product yields and GHG emissions of the process. This approach allows for variations in parameter level values (Supplemental Figure 1) to be included in the uncertainty analysis, along with model uncertainty resulting from the methods used to estimate process data. By drawing on previously reported process data, this method can capture non-normal distributions of process parameters and more accurately describe these distributions. Combined, SA-MCS gives a more holistic overview of uncertainty throughout the entire process.

The pyrolysis modeling process has three main dependencies (Supplemental Figure 2): (1) the relationships and inputs of the pyrolysis model (Table 1), (2) the properties of the biomass feedstock (Supplemental Table 3), and (3) the energy sources and application of the pyrolysis co-products. As the compositional pyrolysis model uses empirical relationships to determine pyrolysis CO_2 and energy fluxes, the distributions of the residuals from the validation of pyrolysis modeling were sampled to account for the uncertainty of the model which was quantified in previous work.[17] Beyond model uncertainty, variation in pyrolysis temperature leads to changes in the pyrolysis product yields, as well as CO_2 and energy fluxes. We then incorporate uncertainty in efficiency factors for the subprocesses within the model, including the pyrolysis process, biomass drying, and the combustion of the different co-products based on the boiler technology used. A complete diagram of model dependencies is given in Supplemental Figure 2.

The second main dependency of the pyrolysis process is related to the composition of the biomass feedstock, specifically the mass-weighted proportions of cellulose, hemicellulose, lignin, and ash. Supplemental Table 3 shows data regarding the possible weighted composition of yellow poplar, which introduces uncertainty into the overall modeling framework.

The final main dependency is related to the energy sources used for the pyrolysis process and the application of co-products. Feedstock drying is examined either using an external energy source (natural gas combustion) or waste heat from the pyrolysis process. Similarly, the actual pyrolysis process could either be powered by the pyrolysis energy products or by an external energy source (e.g., natural gas). Finally, CO_2 and energy fluxes could be affected by how the co-products are used. In this case, bio-oil could either be combusted for energy, combusted without energy recovery, or used as a feedstock for chemical application.

Table 1. List of process emission and energy calculations performed and sources of uncertainty and variation in each calculation parameter. Variables are defined as: *GHG* = greenhouse gas emissions, *m* = mass, *EF* = emission factor, *D* = distance, *f* =mass fraction, η = efficiency factor, ΔH = enthalpy, *T* = temperature, *E* = energy, *Y* = yield, and *C* = carbon content.

Process step	Emission calculation	Sources of uncertainty *	Sources of variation *
Biomass growth **	$GHG_{growth} = \frac{m_{herbicide}}{m_{greenwood}} \cdot EF_{herbicide} + \frac{m_{insecticide}}{m_{greenwood}} \cdot \mathrm{EF}_{insecticide}$	$EF_{herbicide}$ 8.22 - 26.63 kg CO_2e / kg $\mathrm{EF}_{insecticide}$ 14.79 – 18.91 kg CO_2e / kg $m_{herbicide}$ 5.239 kg/ha·yr; 37 – 79 t wood/ha $m_{insecticide}$ 0.03 kg/ha·yr; 37 – 79 t wood/ha	
Harvesting **	$GHG_{harvesting} = \sum_{n=gasoline,\ diesel,\ equip,lubricant} \frac{m_n}{m_{greenwood}} \cdot EF_n$	$EF_{gasoline}$ from [29] EF_{diesel} from [29] EF_{equip} from [32] $EF_{lubricant}$ from [32]	m_n *** Scen. 1 = Chainsaw from [34] Scen. 2 = Feller-buncher from [32]

Transportation	$GHG_{transport} = \left(m_{greenwood} \cdot EF_{transport} \cdot D_{transport}\right) \cdot Allocation$	$EF_{transport}$ 0.157 - 0.169 kg CO_2e / t·km	$D_{transport}$ Scen. 1 = 200-240 km Scen. 2 = 240-280 km
Drying	$GHG_{drying} = f_{moisture} \cdot \Delta H_{drying}/\eta_{drying} \cdot EF_{drying}$	$f_{moisture}$ (see Supplemental Table 3)	EF_{drying} $Scen.\ 1 = Nat.\ gas$ $Scen.\ 2 = Waste\ heat$
Pyrolysis compositional model	**General form (see [17] for exact calculations):** $Outcome_{pyro} = f_{cellulose} \cdot Outcome_{cellulose}(T_{pyro}) + f_{hemicellulose} \cdot Outcome_{hem} + f_{lignin} \cdot Outcome_{lignin}(T_{pyro})$ For outcomes of biochar, syngas, and bio-oil yield, enthalpy, LHV, and carbon content	$f_{cellulose/hemicellulose/lignin}$(see Supplemental Table 3) $Outcome_{pyro}$ Model error calculated from validation residuals (Supplemental Figure 3)	T_{pyro} $Scen.\ 1 = 880 - 900\ °C$ $Scen.\ 2 = 490 - 510\ °C$
Pyrolysis fossil emissions	$\Delta H_{pyro} = Y_{biochar} \cdot \Delta H_{biochar} + Y_{bio-oil} \cdot \Delta H_{bio-oil} + Y_{syngas} \cdot \Delta H_{syngas} - \Delta H_{feedstock}$; $GHG_{pyro\ fossil} = \Delta H_{pyro}/\eta_{pyro} \cdot EF_{pyro}$	ΔH_{pyro} Model error (Supplemental Figure 3)	η_{pyro} Scen. 1 = 85 – 95% Scen. 2 = 45 – 55% EF_{pyro} Scen. 1 = Syngas Scen. 2 = Nat.gas
Pyrolysis biogenic emissions	$GHG_{pyro\ bio} = Y_{bio-oil} \cdot C_{bio-oil} \cdot \frac{44.01}{12.01} \cdot Use\ factor + Y_{syngas} \cdot C_{syngas} \cdot \frac{44.01}{12.01}$	$Y_{bio-oil/syngas}$ Model error (Supplemental Figure 3) $C_{bio-oil/syngas}$ Model error (Supplemental Figure 3)	*Use factor* Scen. 1 = 0% (bio-oil for chemical/material feedstock) Scen. 2 = 100% (bio-oil combusted)
Pyrolysis bound emissions	$GHG_{bound} = Y_{bio-oil} \cdot C_{bio-oil} \cdot \frac{44.01}{12.01} \cdot Use\ factor + Y_{biochar} \cdot C_{biochar} \cdot \frac{44.01}{12.01}$	$C_{bio-oil/biochar}$ Model error (Supplemental Figure 3)	*Use factor* Scen. 1 = 100% (bio-oil for chemical/material feedstock) Scen. 2 = 0% (bio-oil combusted)
Pyrolysis net energy	$E_{net} = LHV_{syngas} \cdot \eta_{syngas} + LHV_{bio-oil} \cdot \eta_{bio-oil} - \frac{\Delta H_{pyro}}{\eta_{pyro}} - E_{drying}$	$\eta_{bio-oil}$*** Scen 1 = 0% (not used for energy) Scen. 2 = 0% (no energy recovery) η_{syngas}*** Scen. 1 = 75-83% Scen. 2 = 0% (no energy recovery)	E_{drying} Scen. 1 = Waste heat (0 MJ energy input) Scen. 2 = Nat. gas

* Variation and uncertainty from upstream factors not shown – see Supplemental Figure 2 for uncertainty and variation dependencies and sub-dependencies.
** See SI for full details.
*** Includes both uncertainty and variation

3. Results

3.1 Deterministic pyrolysis outcomes

Comparing deterministic outputs for both Scenarios, the higher pyrolysis temperature results in a lower biochar yield (22 wt.% vs. 26 wt.%) and bio-oil yield (49 wt.% vs. 53 wt.%) but higher syngas yield (29 wt.% vs. 22 wt.%). However, biochar-bound carbon remains relatively constant at 0.70 kg CO_2 in Scenario 1 relative to 0.73 kg CO_2 in Scenario 2. In Scenario 1, bio-oil carbon is also bound in a chemical product (0.71 kg CO_2), while in Scenario 2 bio-oil is flared. A complete description of deterministic pyrolysis outcomes is given in Supplemental Table 4.

The two Scenarios differ in their treatment of energy inputs and products during pyrolysis (Figure 2). In Scenario 1, 3.62 MJ of energy products are produced, relative to 7.66 MJ consumption in Scenario 2. Those energy requirements in Scenario 2 are met with natural gas, resulting in emissions of 0.39 kg CO_2e representing 53% of the atmospheric CO_2 bound in the biochar.

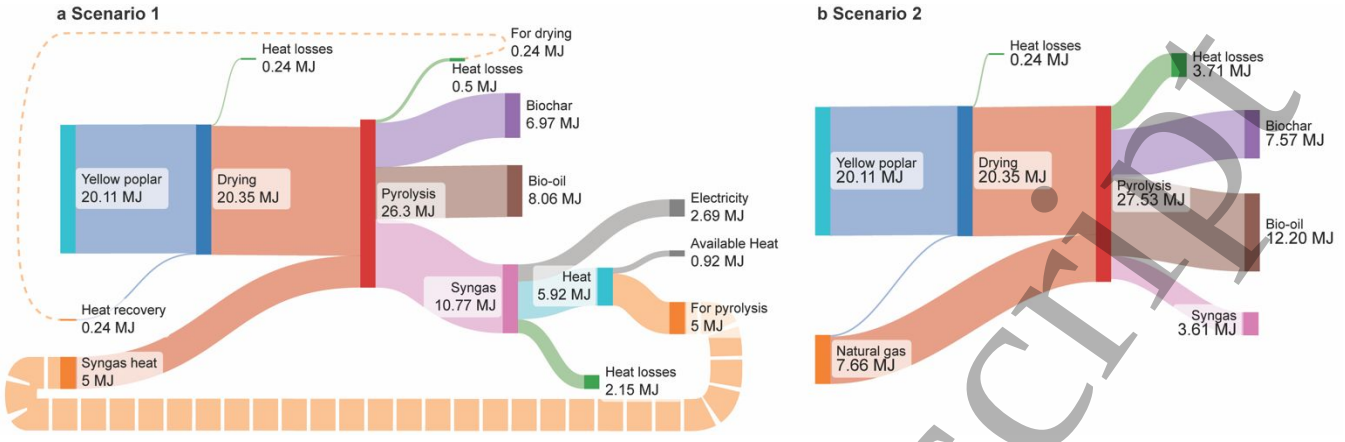

Figure 2. Deterministic energy flow diagram for pyrolysis in (a) Scenario 1 and (b) Scenario 2. Yellow poplar, biochar, bio-oil, and syngas energy are shown as the higher heating values (HHV). Biochar HHV is estimated from the composition.[52] Small imbalances in energy fluxes (e.g., the 4% lower pyrolysis inputs than outputs in Scenario 1) are due to the modeling of the pyrolysis process and product HHVs. Dashed lines represent energy recovery for use in later process units. Note no energy products are utilized in Scenario 2.

3.2 Scenario-Aware Monte Carlo Simulation

For upstream biomass production, the distributions of GHG emissions have a long right tail that signals MCS realizations where lumber production only generates a small mass of residues that can be used for biochar manufacturing (Figure 3a and b). This means that more inputs for biomass growth, harvesting, and transportation are required to yield enough mass of co-products that can be used for pyrolysis. For both processes, Scenario 2 emissions are generally higher than Scenario 1 due to the use of more carbon-intensive harvesting configurations and longer transportation distances.

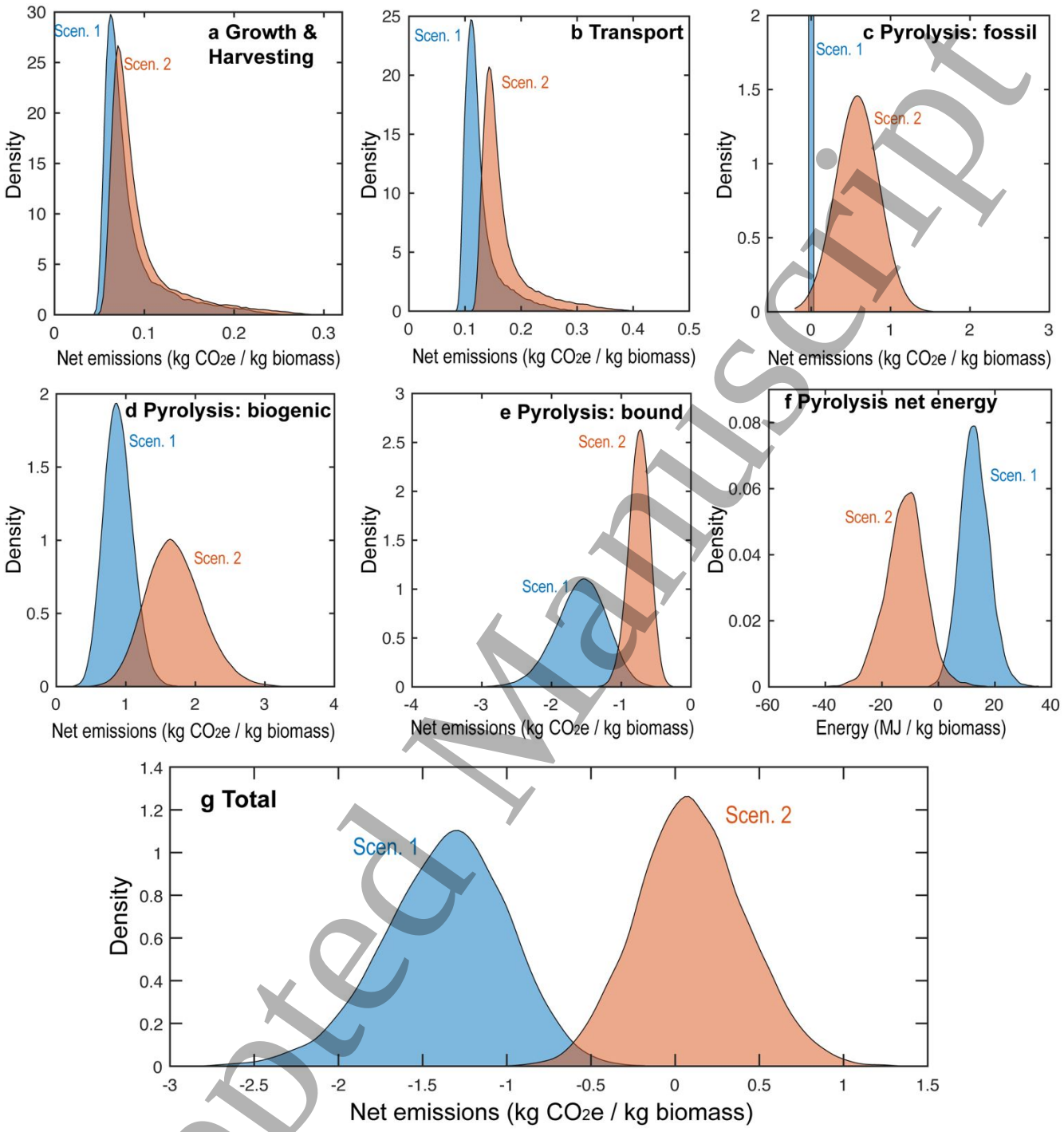

Figure 3. Probability distributions for GHG emissions from (a) biomass feedstock growth and harvesting, (b) biomass feedstock transportation, (c) pyrolysis fossil fuel consumption, (d) pyrolysis from biogenic sources, (e) carbon bound in biochar and bio-oil products during pyrolysis, (f) net energy produced (including heat, electricity, and external energy inputs), and (g) total balance of CO_2e emissions for the two scenarios examined. Negative values represent carbon dioxide removal, while positive values represent emissions.

During pyrolysis, Scenario 1 does not consume any fossil fuels and, therefore, does not lead to any fossil GHG emissions. In Scenario 2, natural gas is used for biomass drying and pyrolysis, which leads to varying fossil GHG emissions (Figure 3c). Certain realizations (1.6% likelihood) in Scenario 2 show

negative fossil GHG emissions, which are cases in which the pyrolysis reaction generates energy. Pyrolysis biogenic emissions are again higher for Scenario 2 relative to Scenario 1 (Figure 3d), due to differences in bio-oil application, with bio-oil combusted without energy recovery in Scenario 2 versus used as a chemical feedstock in Scenario 1. As a result, more biogenic carbon is bound in Scenario 1 than in Scenario 2 (Figure 3e), with a 5-95% range of -1.0 to -2.2 kg CO_2e in Scenario 1 and -0.51 to -1.0 kg CO_2e in Scenario 2.

In total, the two scenarios result in a large difference in total GHG emissions, with a median of -1.4 kg CO_2e for Scenario 1 and +0.090 kg CO_2e for Scenario 2, with distributions that have only a 2.5% overlap. In Scenario 1, it is highly certain that the process will result in carbon removal (>99.99%). In contrast, Scenario 2 is highly uncertain, with a 66% likelihood of net emissions and a 34% likelihood of net CDR.

The net energy balance in Scenario 1 has a median value of 4.4 MJ (5^{th}-95^{th} percentile from -3.5 to 13 MJ), while Scenario 2 results in -11.5 MJ (-23.6 to -0.7 MJ). In Scenario 1, this energy balance is driven by produced electricity with a median of 2.7 MJ (0.7 to 6.3 MJ) and heat with a median of 5.5 MJ (1.4 – 11 MJ), as well as heat consumed for pyrolysis of 4.1 MJ (0.01 – 9.0 MJ). In contrast, Scenario 2 results in no heat or electricity production and consumes 11 MJ of energy for pyrolysis (0.70 - 23 MJ. We note that Scenario 1 GHG emissions do not account for additional emissions in the 18% of the distribution where the net energy is less than zero, and additional energy sources beyond the syngas produced would be needed. The energy produced results in a broader distribution of emissions than other parameters (coefficient of variation of 112% and 103% for Scenario 1 and 2, respectively) because of compounding of model uncertainty through the calculation of pyrolysis energy requirement.

Many past studies assign a GHG emissions credit for avoiding fossil fuel emissions to pyrolysis energy products (Supplemental Table 1). If the energy produced replaced natural gas and electricity at the US grid average,[36] energy credits would reduce GHG emissions by -0.35 kg CO_2e (5^{th}-95^{th} percentile of -1.2 to +0.31 kg CO_2e) in Scenario 1. If included in the total emissions, avoided energy would decrease the total median emissions to -1.7 kg CO_2e. However, we note that these benefits include avoiding emissions rather than removing CO_2, which could be less substantial with future decarbonization of the energy grid.[22] Further, some studies take different approaches to account for this energy product (e.g., system expansion to include biomass combustion[20]), which shifts the benefits of this product.

A key difference between the two Scenarios is the use of bio-oil in a chemical application in Scenario 1, increasing the bound carbon by the carbon content of bio-oil. In Scenario 1, bio-oil bound carbon has a 5^{th}-95^{th} percentile range of -0.35 to -1.42 kg CO_2e, or 34 - 64% of total CDR potential. Importantly, the ability of bio-oil products to result in CDR is highly dependent on the exact product, the product lifespan, and end-of-life scenario of that product. If, instead, bio-oil was combusted in this scenario, net CDR potential would decrease to -0.48 to -0.99 kg CO_2e, and an additional 3.7-6.3 MJ of heat and 1.8 - 3.3 MJ of electricity would be produced (Supplemental Figure 4). This gives bio-oil a median effective emission factor of 0.109 kg CO_2e / MJ, slightly higher than the US electricity average.[36]. In this scenario, 99.8% of the distribution of emissions results in net CDR, demonstrating that CDR is highly certain even while the extent of bio-oil to chemical or material pathways to secure net CDR is uncertain. A second key difference between Scenarios is the use of natural gas as an energy source in Scenario 2, contributing median emissions of 0.57 kg CO_2e (5^{th}-95^{th} percentile of 0.14-1.04 kg CO_2e). At the median, these two factors combined make up 98% of the difference in CDR between Scenario 1 and Scenario 2.

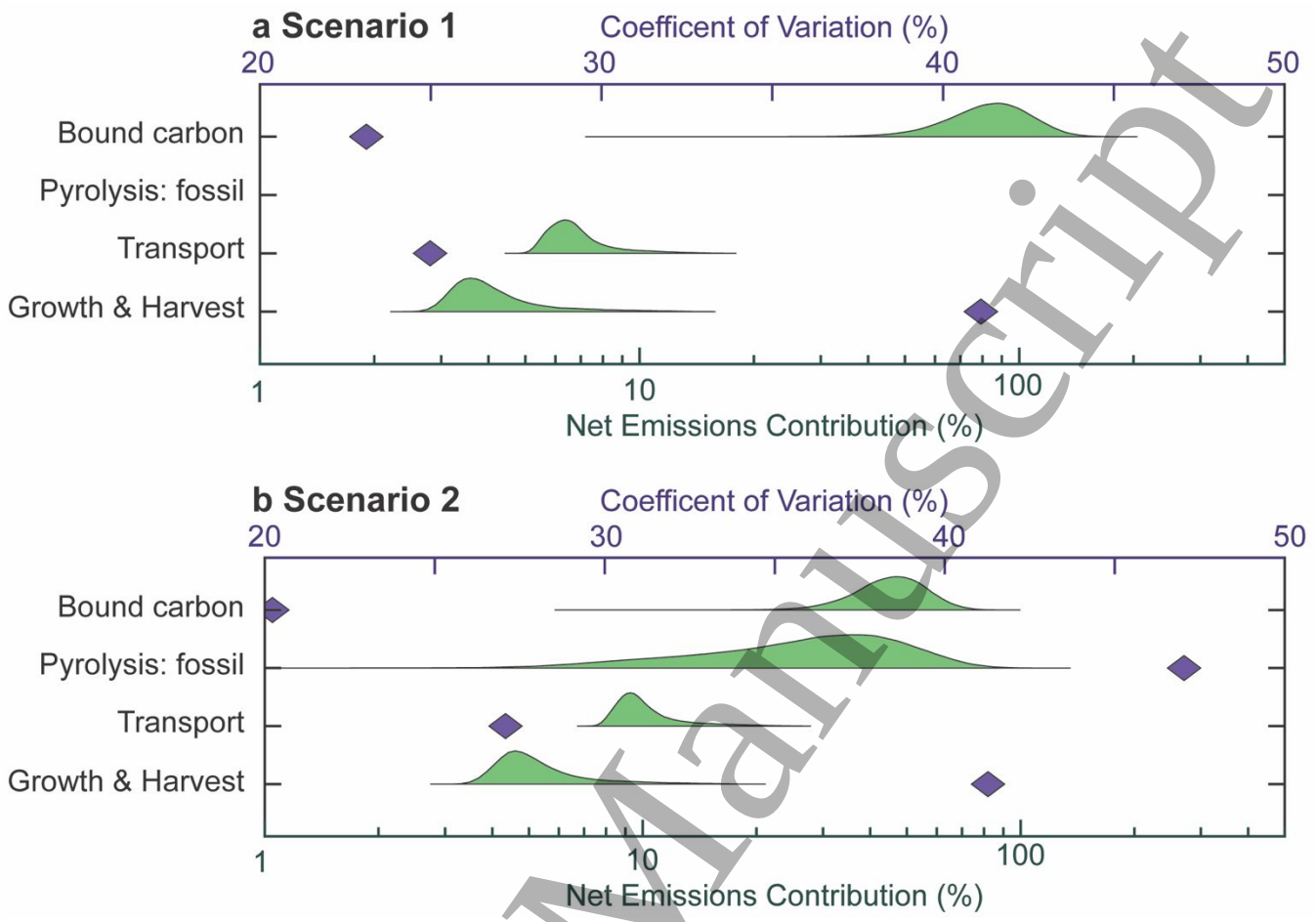

Figure 4. Coefficient of variation and CO_2e emissions contribution for each process step for (a) Scenario 1 and (b) Scenario 2. Totals may not sum to 100% due to the mixture of positive and negative contributions.

The total GHG emissions of pyrolysis are relatively insensitive to uncertainty in growth/ harvesting and transport emissions, despite high coefficients of variation, with median contributions of 4.1% and 6.7% in Scenario 1 and 5.2% and 9.9% in Scenario 2 (Figure 4). In contrast, in both Scenarios, total emissions are highly sensitive to changes in bound carbon content, but this category shows a relatively narrow distribution. In Scenario 2, emissions due to fossil fuel inputs to meet the energy requirement of pyrolysis both make up a high contribution of total emissions (median of 37%) and show a broad distribution (coefficient of variation of 47%).

In this analysis, emissions from biomass growth/harvesting and transportation were allocated to the biomass residue feedstock on a mass basis. If, instead, no transportation or growth/harvesting emissions were assigned to residue feedstocks, net CDR would decrease to a median of -1.55 and -0.17 kg CO_2 in Scenario 1 and 2, respectively. Notably, while this is only a 10.7% increase in net CDR in Scenario 1, in Scenario 2, no allocation of transport and growth/harvesting emissions shifts the median emissions from net emitting to net removal. With this allocation, Scenario 2 has a 67% likelihood of removal and a 33% likelihood of emissions. This shift in median highlights that when net GHG emissions are near zero, allocation assumptions can meaningfully shift median GHG fluxes, but net removal in these scenarios is still uncertain.

4. Discussion

The two Scenarios represent likely real-world maxima and minima CDR of biomass pyrolysis. As such, it is not unexpected that all reviewed LCA data (academic: -0.05 to -1.45 kg CO_2e, Supplemental Table 1 and commercial: -0.22 to -1.2 kg CO_2e, Supplemental Table 2) fall between the medians of the two Scenarios. However, in the alternative Scenario 1 with bio-oil combustion, the median is -0.52 kg CO_2e (5^{th}-9^{th} percentile of -0.24 to -0.80 kg CO_2e, Supplemental Figure 4), which is well aligned with previous data at pyrolysis temperatures of ≥ 500 °C from residue biomass (median of -0.64 kg CO_2e and a 5^{th}-95^{th} percentile range of -0.22 to -0.80 kg CO_2e) and industry CDR data (Supplemental Table 2). As bio-oil to chemical processes are currently not widespread,[53] combustion of bio-oil or bio-oil sequestration via underground injection[54] are more likely pathways for the use of this material at present.

Herein, all emissions are allocated to the biochar product, with no emissions allocated to produced energy. The inclusion of a GHG credit for energy products (e.g., the median of -0.35 kg CO_2e in Scenario 1, as calculated in Section 3) would introduce additional uncertainty surrounding regional and temporal[55] variation in energy emission intensity. The emission intensity of electricity production is expected to decrease over time, but meaningful uncertainty exists in how fast this decarbonization will occur, introducing variation and uncertainty surrounding the replacement of energy products with pyrolysis co-products over the lifespan of a pyrolysis plant.

Recent industry reports for biochar production show that 37% of global producers use continuous processes, whereas 45% use batch or mobile processes.[13] Only 26% of producers report recapturing energy products to produce electricity, whereas 31% of producers report using their energy co-products to fuel pyrolysis. As the use of fossil fuel energy sources for pyrolysis was identified as a key factor in higher emissions in Scenario 2 than in Scenario 1, and continuous processes would be expected to be more efficient than batch processes,[56] this work highlights that the CDR potential of many existing commercial biochar operations is highly uncertain. The commercial data used as a comparison in this work (Supplemental Table 2) relied on reporting to comply with CDR markets, which have standards that prohibit the use of fossil fuel inputs for pyrolysis. Therefore, it is likely that the 69% of producers that do not report using energy co-products to fuel pyrolysis results in distributions of GHG emissions more similar to Scenario 2 than to existing public, commercial data. As available LCA data focuses on high-efficiency and low emission processes, CDR of producers with less efficient processes may be overestimated.

In the "poor practices" Scenario 2, natural gas was examined as the fuel source for pyrolysis. In previous assessments, biomass and electricity have been more commonly examined as energy inputs for pyrolysis (Supplemental Table 1). Emission factors for biomass-to-energy are highly variable,[57] and emission factors for electricity are highly spatially variable. Therefore, it is likely that assessment of these energy sources would increase uncertainty in biochar CDR, as no uncertainty in natural gas emission factor was considered herein.

4.1 Limitations

The cradle-to-gate scope of the analysis herein excludes the application phase. However, biochar can provide significant additional environmental benefits during the use phase in applications such as agricultural soil amendment [6–8,58], cement replacement,[9,10] and plastic additive.[11,12] These benefits are variable between applications[18] and locations[59] and, for many applications, are expected to be highly uncertain. For example, wide ranges of strength outcomes for biochar in concrete have been reported and limited data on the durability of biochar-concrete composites exists, resulting in increased uncertainty.[10] In agricultural soil amendment applications, factors such as high geospatial variation, uncertainty surrounding long-term impacts of biochar addition to soil, variation in impacts depending on

the crop grown, and uncertainty surrounding future fertilizer decarbonization contribute to this uncertainty.[58,60]

In addition to benefits during application, biochar stability may vary between applications, locations, and with biochar properties.[35] As a result, a portion of the bound carbon in biochar may oxidize to CO_2, reducing the CDR of biochar over the cradle-to-gate analysis presented here. When considering the biochar produced in Scenario 1 and 2, the median bound carbon at the factory gate is 0.72 kg CO_2e and 0.74 kg CO_2e, respectively. When applying the model developed by Budai et al.[61] for biochar carbon stability in soil over 100 years, this is reduced to 0.68 and 0.56 kg CO_2e for Scenario 1 and 2, respectively. Notably, despite less biochar bound carbon at the factory gate, Scenario 1 results in more bound carbon after 100 years with this model due to the lower H/C atomic ratio resulting from higher pyrolysis temperatures. Additionally, biochar stability is expected to vary by application; however, no studies were identified that examine biochar stability in applications other than soil amendment.

The distributions of data resulting from this analysis could be narrowed if more facility-specific processes and LCI data for commercial pyrolysis processes were available. Thermal efficiency is a particularly important data gap, with no facility-specific thermal efficiency data identified in the literature. Understanding thermal efficiency is key to understanding whether the heat produced via pyrolysis co-products is sufficient to meet the energy needs of pyrolysis, which was identified as a key factor in maximizing net CDR. The analysis of uncertainty herein highlights the importance of considering uncertainty when estimating LCI data, particularly across the biochar industry as a whole, and gives an understanding of how variation in industrial practices can impact net CDR, even in the absence of facility-specific data.

4.2 Policy and Industrial Impact

Projections suggest 2,700 kt of biochar will be produced worldwide by 2025.[13] To give context for scale, if this magnitude of biochar were produced with Scenario 1, -24 to -9.6 Mt CO_2e of CDR would be achieved, while if Scenario 2 were used, the range would be from -4.5 to +6.8 Mt CO_2e. We note that this does not account for variations in feedstock or local variations in transportation emissions or energy grids. The data presented herein can inform future industry growth via the selection of process parameters that are highly likely to secure net CDR, primarily avoiding the use of non-renewable fuel sources and maximizing thermal efficiency and use of fuel co-products. At a policy level, this work can inform ongoing efforts to develop and adopt standards for biochar CDR that ensure high confidence in net removal when accounting for broad variation and uncertainty in facility-specific practices. Current standards for biochar CDR (e.g., the European Biochar Certificate[62] and World Biochar Certificate[63]) prohibit the use of fossil fuel energy sources and specify a minimum energy recovery of 70% of co-product energy content. Scenario 2 does not meet the energy sourcing or efficiency requirements due to its use of natural gas and low energy recovery, and CDR is uncertain in this scenario. Of the scenarios examined, the alternative Scenario 1 with bio-oil combustion (Supplemental Figure 4) is closest to this minimum (but with higher thermal efficiency) and has a >99% likelihood of net CDR.

Beyond what is modeled herein, inefficient system designs may be more likely to emit methane present in syngas to the environment.[65] If all of the methane produced in Scenario 1 were released to the environment, net GHG emissions would increase by a median of 0.37 kg CO_2e. To maximize the CDR potential of biochar, it is critical to ensure that all producers are utilizing efficiently designed systems to avoid any unintended emissions from biochar production. This finding may be particularly applicable for mobile or small-scale pyrolysis units that are transported to the location of the feedstock; care should be taken to examine tradeoffs between transportation emissions, pyrolysis efficiency, and energy capture

against the potential benefits of mobile pyrolysis, such as forest fire fuel reduction and reduced biomass transportation distances.[64]

5. Conclusions

Understanding the uncertainty inherent in the life-cycle data of pyrolysis is critical to informing the CDR potential of biochar, particularly when LCI data are estimated with modeling approaches. As the biochar industry continues to expand, focus should be placed on energy efficiency and the recapture of pyrolysis energy products, as well as data availability and standardization (e.g., EPDs), which can aid in narrowing uncertainty distributions and inform policy and industry development. The development of economical processes to produce currently fossil fuel-derived products from bio-oil, allowing for additional carbon sequestration of bio-oil carbon, is key to maximizing the CDR potential of waste biomass resources, particularly in future scenarios with decarbonized energy grids. To maximize the likelihood of net carbon removal, biochar producers should ensure that fossil fuel energy inputs are not used, syngas and bio-oil products are used to offset petroleum-derived energy or chemicals, and pyrolysis systems are efficiently designed. Ensuring that producers meet existing standards and guidelines for biochar production and expanding the acceptance of these standards is critical to avoiding unintended carbon dioxide emissions from pyrolysis.

Acknowledgments

Funding for this work was provided by the US Department of Energy, Advanced Research Projects Agency–Energy (ARPA-E, Grant #DE-AR0001625). For authors affiliated with LBNL, this project was also funded by the DOE Office of Technology Transitions in collaboration with the Office of Clean Energy Demonstrations (OCED), the Office of Fossil Energy and Carbon Management (FECM), and Bioenergy Technologies Office (BETO), US Department of Energy through Contract DE-AC02-05CH11231 between Lawrence Berkeley National Laboratory and the US Department of Energy. The views expressed in the article do not necessarily represent the views of the US government. The US government retains, and the publisher, by accepting the article for publication, acknowledges, that the US government retains a nonexclusive, paid, irrevocable, worldwide license to publish or reproduce the published form of this manuscript, or allow others to do so, for US government purposes.

Conflicts of interest

C. D. S. has a financial interest in Cyklos Materials. Cyklos Materials has no financial interest or relationship to this work. All other authors have no conflicts of interest to declare.

References

(1) Intergovernmental Panel on Climate Change. *Climate Change 2023 Synthesis Report*; 2023. doi.org/ 10.59327/IPCC/AR6-9789291691647.

(2) CDR.fyi. *CDR.fyi 2022 Year in Review*. CDR-fyi. https://medium.com/cdr-fyi/cdr-fyi-2022-year-in-review-d095acd9a1a0 (accessed 2023-09-16).

(3) Chiaramonti, D.; Lehmann, J.; Berruti, F.; Giudicianni, P.; Sanei, H.; Masek, O. Biochar Is a Long-Lived Form of Carbon Removal, Making Evidence-Based CDR Projects Possible. *Biochar* **2024**, *6* (1), 81. https://doi.org/10.1007/s42773-024-00366-7.

(4) National Academies of Sciences; Division on Earth; Life Studies; Ocean Studies Board; Board on Chemical Sciences; Board on Earth Sciences; Board on Energy; Environmental Systems; Board on

Atmospheric Sciences; Committee on Developing a Research Agenda for Carbon Dioxide Removal. Negative Emissions Technologies and Reliable Sequestration: A Research Agenda. **2019**.

(5) Intergovernmental Panel on Climate Change. *Emissions Gap Report 2023*; 2023. https://doi.org/10.59117/20.500.11822/43922.

(6) Roberts, K. G.; Gloy, B. A.; Joseph, S.; Scott, N. R.; Lehmann, J. Life Cycle Assessment of Biochar Systems: Estimating the Energetic, Economic, and Climate Change Potential. *Environmental Science and Technology* **2010**, *44* (2), 827–833. https://doi.org/10.1021/es902266r.

(7) Woolf, D.; Amonette, J. E.; Street-Perrott, F. A.; Lehmann, J.; Joseph, S. Sustainable Biochar to Mitigate Global Climate Change. *Nat Commun* **2010**, *1* (1), 56. https://doi.org/10.1038/ncomms1053.

(8) Matuštík, J.; Hnátková, T.; Kočí, V. Life Cycle Assessment of Biochar-to-Soil Systems: A Review. *Journal of Cleaner Production* **2020**, *259*, 120998. https://doi.org/10.1016/J.JCLEPRO.2020.120998.

(9) Campos, J.; Fajilan, S.; Lualhati, J.; Mandap, N.; Clemente, S. Life Cycle Assessment of Biochar as a Partial Replacement to Portland Cement. *IOP Conference Series: Earth and Environmental Science* **2020**, *479* (1), 012025. https://doi.org/10.1088/1755-1315/479/1/012025.

(10) Zhao, Z.; El-Naggar, A.; Kau, J.; Olson, C.; Tomlinson, D.; Chang, S. X. Biochar Affects Compressive Strength of Portland Cement Composites: A Meta-Analysis. *Biochar* **2024**, *6* (1), 21. https://doi.org/10.1007/s42773-024-00309-2.

(11) Kane, S.; Van Roijen, E.; Ryan, C.; Miller, S. Reducing the Environmental Impacts of Plastics While Increasing Strength: Biochar Fillers in Biodegradable, Recycled, and Fossil-Fuel Derived Plastics. *Composites Part C: Open Access* **2022**, *8*, 100253. https://doi.org/10.1016/j.jcomc.2022.100253.

(12) Roy, P.; Defersha, F.; Rodriguez-Uribe, A.; Misra, M.; Mohanty, A. K. Evaluation of the Life Cycle of an Automotive Component Produced from Biocomposite. *Journal of Cleaner Production* **2020**, *273*, 123051. https://doi.org/10.1016/j.jclepro.2020.123051.

(13) International Biochar Initative. *Global Biochar Market Report*; 2024. https://biochar-international.org/2023-global-biochar-market-report/.

(14) Peters, J. F.; Iribarren, D.; Dufour, J. Biomass Pyrolysis for Biochar or Energy Applications? A Life Cycle Assessment. *Environmental Science and Technology* **2015**, *49* (8), 5195–5202. https://doi.org/10.1021/ES5060786/SUPPL_FILE/ES5060786_SI_001.PDF.

(15) Rajabi Hamedani, S.; Kuppens, T.; Malina, R.; Bocci, E.; Colantoni, A.; Villarini, M. Life Cycle Assessment and Environmental Valuation of Biochar Production: Two Case Studies in Belgium. *Energies* **2019**, *12* (11), 2166. https://doi.org/10.3390/en12112166.

(16) Azzi, E. S.; Karltun, E.; Sundberg, C. Prospective Life Cycle Assessment of Large-Scale Biochar Production and Use for Negative Emissions in Stockholm. *Environ. Sci. Technol.* **2019**, *53* (14), 8466–8476. https://doi.org/10.1021/acs.est.9b01615.

(17) Kane, S.; Miller, S. A. Predicting Biochar Properties and Pyrolysis Life-Cycle Inventories with Compositional Modeling. *Bioresource Technology* **2024**, *399*, 130551. https://doi.org/10.1016/j.biortech.2024.130551.

(18) Azzi, E. S.; Karltun, E.; Sundberg, C. Life Cycle Assessment of Urban Uses of Biochar and Case Study in Uppsala, Sweden. *Biochar* **2022**, *4* (1), 18. https://doi.org/10.1007/s42773-022-00144-3.

(19) Lefebvre, D.; Williams, A.; Kirk, G. J. D.; Meersmans, J.; Sohi, S.; Goglio, P.; Smith, P. An Anticipatory Life Cycle Assessment of the Use of Biochar from Sugarcane Residues as a Greenhouse Gas Removal Technology. *Journal of Cleaner Production* **2021**, *312*, 127764. https://doi.org/10.1016/j.jclepro.2021.127764.

(20) Brassard, P.; Godbout, S.; Hamelin, L. Framework for Consequential Life Cycle Assessment of Pyrolysis Biorefineries: A Case Study for the Conversion of Primary Forestry Residues. *Renewable and Sustainable Energy Reviews* **2021**, *138*, 110549. https://doi.org/10.1016/j.rser.2020.110549.

(21) Muñoz, E.; Curaqueo, G.; Cea, M.; Vera, L.; Navia, R. Environmental Hotspots in the Life Cycle of a Biochar-Soil System. *Journal of Cleaner Production* **2017**, *158*, 1–7. https://doi.org/10.1016/j.jclepro.2017.04.163.
(22) Azzi, E. S.; Li, H.; Cederlund, H.; Karltun, E.; Sundberg, C. Modelling Biochar Long-Term Carbon Storage in Soil with Harmonized Analysis of Decomposition Data. *Geoderma* **2024**, *441*, 116761. https://doi.org/10.1016/j.geoderma.2023.116761.
(23) Peng, L.; Searchinger, T. D.; Zionts, J.; Waite, R. The Carbon Costs of Global Wood Harvests. *Nature* **2023**, *620* (7972), 110–115. https://doi.org/10.1038/s41586-023-06187-1.
(24) Liao, M.; Kelley, S.; Yao, Y. Generating Energy and Greenhouse Gas Inventory Data of Activated Carbon Production Using Machine Learning and Kinetic Based Process Simulation. *ACS Sustainable Chem. Eng.* **2020**, *8* (2), 1252–1261. https://doi.org/10.1021/acssuschemeng.9b06522.
(25) Parvatker, A. G.; Eckelman, M. J. Comparative Evaluation of Chemical Life Cycle Inventory Generation Methods and Implications for Life Cycle Assessment Results. *ACS Sustainable Chem. Eng.* **2019**, *7* (1), 350–367. https://doi.org/10.1021/acssuschemeng.8b03656.
(26) puro.earth. *Puro Standard: Biochar Methodology Edition 2022 V3*; 2024. https://fs.hubspotusercontent00.net/hubfs/7518557/Supplier%20Documents/Puro.earth%20Biochar%20Methodology.pdf.
(27) EPD International. *Biochar Product Category Classification: UN CPC 345*; Product Category Rules; 2021.
(28) Miller, S. A. The Role of Data Variability and Uncertainty in the Probability of Mitigating Environmental Impacts from Cement and Concrete. *Environmental Research Letters* **2021**, *16* (5), 054053. https://doi.org/10.1088/1748-9326/ABE677.
(29) Bin Thaneya, A.; Gursel, A. P.; Kane, S.; Miller, S. A.; Horvath, A. Assessing Uncertainty in Building Material Emissions Using Scenario-Aware Monte Carlo Simulation. *Environ. Res.: Infrastruct. Sustain.* **2024**. https://doi.org/10.1088/2634-4505/ad40ce.
(30) Miller, S. A.; Van Roijen, E.; Cunningham, P. R.; Kim, A. Opportunities and Challenges for Engineering Construction Materials as Carbon Sinks. *RILEM Technical Letters* **2021**, *6*, 105–118. https://doi.org/10.21809/RILEMTECHLETT.2021.146.
(31) Morales-Vera, R.; Vásquez-Ibarra, L.; Scott, F.; Puettmann, M.; Gustafson, R. Life Cycle Assessment of Bioethanol Production: A Case Study from Poplar Biomass Growth in the U.S. Pacific Northwest. *Fermentation* **2022**, *8* (12). https://doi.org/10.3390/fermentation8120734.
(32) Abbas, D.; Handler, R. M. Life-Cycle Assessment of Forest Harvesting and Transportation Operations in Tennessee. *Journal of Cleaner Production* **2018**, *176*, 512–520. https://doi.org/10.1016/j.jclepro.2017.11.238.
(33) Argonne National Laboratory. *Greenhouse Gases, Regulated Emissions, and Energy Use in Technologies (GREET)*; US Dept. of Energy, 2023. https://greet.anl.gov/.
(34) National Renewable Energy Laboratory. United States Life Cycle Inventory Database, 2012. https://www.lcacommons.gov/nrel/search.
(35) Leng, L.; Xu, X.; Wei, L.; Fan, L.; Huang, H.; Li, J.; Lu, Q.; Li, J.; Zhou, W. Biochar Stability Assessment by Incubation and Modelling: Methods, Drawbacks and Recommendations. *Science of The Total Environment* **2019**, *664*, 11–23. https://doi.org/10.1016/j.scitotenv.2019.01.298.
(36) United States Environmental Protection Agency. Emissions & Generation Resource Integrated Database (eGRID), 2023. https://www.epa.gov/egrid.
(37) van den Broek, R.; Faaij, A.; van Wijk, A. Biomass Combustion for Power Generation. *Biomass and Bioenergy* **1996**, *11* (4), 271–281. https://doi.org/10.1016/0961-9534(96)00033-5.
(38) Bridgwater, A. V. The Technical and Economic Feasibility of Biomass Gasification for Power Generation. *Fuel* **1995**, *74* (5), 631–653. https://doi.org/10.1016/0016-2361(95)00001-L.

(39) Shafie, S. M.; Mahlia, T. M. I.; Masjuki, H. H.; Ahmad-Yazid, A. A Review on Electricity Generation Based on Biomass Residue in Malaysia. *Renewable and Sustainable Energy Reviews* **2012**, *16* (8), 5879–5889. https://doi.org/10.1016/j.rser.2012.06.031.

(40) Dasappa, S.; Subbukrishna, D. N.; Suresh, K. C.; Paul, P. J.; Prabhu, G. S. Operational Experience on a Grid Connected 100 kWe Biomass Gasification Power Plant in Karnataka, India. *Energy for Sustainable Development* **2011**, *15* (3), 231–239. https://doi.org/10.1016/j.esd.2011.03.004.

(41) McKendry, P. Energy Production from Biomass (Part 1): Overview of Biomass. *Bioresource Technology* **2002**, *83* (1), 37–46. https://doi.org/10.1016/S0960-8524(01)00118-3.

(42) Ahrenfeldt, J.; Henriksen, U.; Jensen, T. K.; Gøbel, B.; Wiese, L.; Kather, A.; Egsgaard, H. Validation of a Continuous Combined Heat and Power (CHP) Operation of a Two-Stage Biomass Gasifier. *Energy Fuels* **2006**, *20* (6), 2672–2680. https://doi.org/10.1021/ef0503616.

(43) Assanee, N.; Boonwan, C. State of The Art of Biomass Gasification Power Plants in Thailand. *Energy Procedia* **2011**, *9*, 299–305. https://doi.org/10.1016/j.egypro.2011.09.032.

(44) Wu, C. Z.; Huang, H.; Zheng, S. P.; Yin, X. L. An Economic Analysis of Biomass Gasification and Power Generation in China. *Bioresource Technology* **2002**, *83* (1), 65–70. https://doi.org/10.1016/S0960-8524(01)00116-X.

(45) Zhou, Z.; Yin, X.; Xu, J.; Ma, L. The Development Situation of Biomass Gasification Power Generation in China. *Energy Policy* **2012**, *51*, 52–57. https://doi.org/10.1016/j.enpol.2012.05.085.

(46) Bang-Møller, C.; Rokni, M. Thermodynamic Performance Study of Biomass Gasification, Solid Oxide Fuel Cell and Micro Gas Turbine Hybrid Systems. *Energy Conversion and Management* **2010**, *51* (11), 2330–2339. https://doi.org/10.1016/j.enconman.2010.04.006.

(47) Faaij, A.; van Ree, R.; Waldheim, L.; Olsson, E.; Oudhuis, A.; van Wijk, A.; Daey-Ouwens, C.; Turkenburg, W. Gasification of Biomass Wastes and Residues for Electricity Production. *Biomass and Bioenergy* **1997**, *12* (6), 387–407. https://doi.org/10.1016/S0961-9534(97)00010-X.

(48) Ståhl, K.; Neergaard, M. IGCC Power Plant for Biomass Utilisation, Värnamo, Sweden. *Biomass and Bioenergy* **1998**, *15* (3), 205–211. https://doi.org/10.1016/S0961-9534(98)00025-7.

(49) Leme, M. M. V.; Venturini, O. J.; Lora, E. E. S.; Rocha, M. H.; Luz, F. C.; Almeida, W. de; de Moura, D. C.; de Moura, L. F. Electricity Generation from Pyrolysis Gas Produced in Charcoal Manufacture: Technical and Economic Analysis. *Journal of Cleaner Production* **2018**, *194*, 219–242. https://doi.org/10.1016/j.jclepro.2018.05.101.

(50) All Power Labs. *Power Pallet PP30 Data Sheet*; 2023. https://www.allpowerlabs.com/wp-content/uploads/2019/08/PP30OneSheet2_1_23-2.pdf.

(51) International Energy Agency. *Thermal Gasification of Biomass*; 2013. https://www.ieabioenergy.com/wp-content/uploads/2013/10/18_AR1999Task20colour.pdf.

(52) Qian, C.; Li, Q.; Zhang, Z.; Wang, X.; Hu, J.; Cao, W. Prediction of Higher Heating Values of Biochar from Proximate and Ultimate Analysis. *Fuel* **2020**, *265*, 116925. https://doi.org/10.1016/j.fuel.2019.116925.

(53) Hu, X.; Gholizadeh, M. Progress of the Applications of Bio-Oil. *Renewable and Sustainable Energy Reviews* **2020**, *134*, 110124. https://doi.org/10.1016/j.rser.2020.110124.

(54) Erica L. Belmont; Julio Friedmann; Matthew Potts; Daniel Sanchez; Roxby Hartley; Salman Khan; Andrew Schaper. *Bio-Oil Injection: Prototype Protocol for Measurement, Reporting, and Verification*; Charm Industrial. https://charmindustrial.com/Bio-oil_Sequestration__Protocol_for_Measurement_Reporting_and_Verification.pdf.

(55) Tian, X.; An, C.; Chen, Z. The Role of Clean Energy in Achieving Decarbonization of Electricity Generation, Transportation, and Heating Sectors by 2050: A Meta-Analysis Review. *Renewable and Sustainable Energy Reviews* **2023**, *182*, 113404. https://doi.org/10.1016/j.rser.2023.113404.

(56) Mong, G. R.; Chong, C. T.; Chong, W. W. F.; Ng, J.-H.; Ong, H. C.; Ashokkumar, V.; Tran, M.-V.; Karmakar, S.; Goh, B. H. H.; Mohd Yasin, M. F. Progress and Challenges in Sustainable Pyrolysis Technology: Reactors, Feedstocks and Products. *Fuel* **2022**, *324*, 124777. https://doi.org/10.1016/j.fuel.2022.124777.

(57) Bhatt, A.; Ravi, V.; Zhang, Y.; Heath, G.; Davis, R.; Tan, E. C. D. Emission Factors of Industrial Boilers Burning Biomass-Derived Fuels. *Journal of the Air & Waste Management Association* **2023**, *73* (4), 241–257. https://doi.org/10.1080/10962247.2023.2166158.

(58) Dokoohaki, H.; Miguez, F. E.; Laird, D.; Dumortier, J. Where Should We Apply Biochar? *Environ. Res. Lett.* **2019**, *14* (4), 044005. https://doi.org/10.1088/1748-9326/aafcf0.

(59) Jeffery, S.; Abalos, D.; Prodana, M.; Bastos, A. C.; Groenigen, J. W. van; Hungate, B. A.; Verheijen, F. Biochar Boosts Tropical but Not Temperate Crop Yields. *Environ. Res. Lett.* **2017**, *12* (5), 053001. https://doi.org/10.1088/1748-9326/aa67bd.

(60) El-Naggar, A.; Lee, S. S.; Rinklebe, J.; Farooq, M.; Song, H.; Sarmah, A. K.; Zimmerman, A. R.; Ahmad, M.; Shaheen, S. M.; Ok, Y. S. Biochar Application to Low Fertility Soils: A Review of Current Status, and Future Prospects. *Geoderma* **2019**, *337*, 536–554. https://doi.org/10.1016/j.geoderma.2018.09.034.

(61) Budai, A.; Zimmerman, A. R.; Cowie, A. L.; Webber, J. B. W.; Singh, B. P.; Glaser, B.; Masiello, C. A.; Shields, F.; Lehmann, J.; Arbestain, M. C.; Williams, M.; Sohi, S.; Joseph, S. Biochar Carbon Stability Test Method: An Assessment of Methods to Determine Biochar Carbon Stability.

(62) Carbon Standards International. European Biochar Certificate - Guidelines for a Sustainable Production of Biochar, 2022. http://european-biochar.org/.

(63) Carbon Standards International. Global Biochar Certificate - Guidelines for a Sustainable Production of Biochar and Its Certification, 2023. european-biochar.org.

(64) Badger, P. C.; Fransham, P. Use of Mobile Fast Pyrolysis Plants to Densify Biomass and Reduce Biomass Handling Costs—A Preliminary Assessment. *Biomass and Bioenergy* **2006**, *30* (4), 321–325. https://doi.org/10.1016/j.biombioe.2005.07.011.